Journal of Catalysis **192,** 108–118 (2000)
doi:10.1006/jcat.2000.2816, available online at http://www.idealibrary.com on IDEAL®

Palladium–Silver Sol–Gel Catalysts for Selective Hydrodechlorination of 1,2-Dichloroethane into Ethylene

II. Surface Composition of Alloy Particles

Benoît Heinrichs,* Francis Noville,* Jean-Paul Schoebrechts,† and Jean-Paul Pirard*

**Laboratoire de Génie Chimique, B6a, Université de Liège, B-4000 Liège, Belgium; and* †*Laboratoire Central,*
Solvay, S.A., Rue de Ransbeek, 310, B-1120 Brussels, Belgium
E-mail: b.heinrichs@ulg.ac.be

Received September 16, 1999; revised January 5, 2000; accepted January 5, 2000

The surface composition of alloy particles in Pd–Ag/SiO$_2$ hydrodechlorination (HDC) sol–gel catalysts has been determined by combining three experimental techniques, carbon monoxide chemisorption, X-ray diffraction, and transmission electron microscopy. Values obtained through this method show a very marked silver enrichment of the surface, as expected: as a consequence of the important gap between palladium and silver surface energies. These values are in complete agreement with surface composition curves calculated in other studies by means of Auger electron spectroscopy and infrared spectroscopy. The influence of sample pretreatment temperature as well as the influence of carbon monoxide on surface composition are discussed.

Key Words: **Pd–Ag alloys; surface composition; CO chemisorption; sol–gel catalysts; hydrodechlorination.**

INTRODUCTION

The surface composition of alloys can strongly deviate from their bulk composition (1, 2). In the case of the palladium–silver alloy, this composition gap between surface and bulk has been shown by several authors. Kuijers and Ponec (3) determined the surface composition of several Pd–Ag alloys from Auger electron spectroscopy. The values they obtained indicate a very marked surface enrichment with silver. These authors also calculated surface composition from infrared spectroscopy results of carbon monoxide adsorbed on Pd–Ag/SiO$_2$ catalysts (4, 5). Values obtained in this way confirm the alloy surface enrichment with silver. The results of Kuijers and Ponec are in agreement with earlier studies of Pd–Ag alloys by Auger spectroscopy (6), photoelectron emission (7), and adsorption and thermal desorption of carbon monoxide (8), which show qualitatively that the silver concentration at the surface of Pd–Ag alloys is higher than its concentration in the bulk.

From the thermodynamic point of view, surface enrichment with silver is foreseeable. It results indeed from the important gap between the surface energies σ of palladium and silver. Surface energies vary with temperature, the minimum value corresponding to the melting point (1814 K for Pd and 1234 K for Ag (2)) and the maximum value corresponding to 0 K. With palladium, values of surface energy σ_{Pd} belong to the interval 1.74 J m$^{-2} \leq \sigma_{\mathrm{Pd}} \leq$ 2.00 J m^{-2} between melting temperature and 0 K. With silver, this interval is 1.09 J m$^{-2} \leq \sigma_{\mathrm{Ag}} \leq$ 1.24 J m^{-2} (9). The lower surface energy of silver favors the surface enrichment of the alloy with this metal (10).

In the first paper of this series (11), the synthesis of Pd–Ag/SiO$_2$ catalysts by a sol–gel procedure is described, in which the preparation of the support and the distribution of the active metals' precursors in the porosity are gathered in a single step. The resultant catalysts contain small Pd–Ag crystallites ($\leq$3 nm) trapped inside 10- to 20-nm microporous silica particles, themselves arranged in larger aggregates. Some large pure silver crystallites are also observed outside silica particles. When the silver content is high enough, those catalysts convert 1,2-dichloroethane into C$_2$H$_4$ with a high selectivity, to the detriment of C$_2$H$_6$ (11–13).

An important purpose of the overall study presented in this series of papers is the understanding of the mechanism of selective hydrodechlorination (HDC) of 1,2-dichloroethane into ethylene on a supported Pd–Ag alloy. To this end, it is desirable to obtain information on the composition of the surfaces where hydrodechlorination and associated hydrogenation occur. The objective of the present paper is to propose an experimental method for determining the surface composition of Pd–Ag alloy particles in the above-mentioned catalysts and compare our results with those published in the literature and obtained with other methods.

0021-9517/00 $35.00

EXPERIMENTAL

I. Catalyst Preparation

The three bimetallic catalysts Pd–Ag/SiO_2 as well as the monometallic catalyst Ag/SiO_2 examined in this paper are xerogels prepared by a one-step sol–gel procedure which consists in the cogelation of the silica precursor, tetraethoxysilane (TEOS), with organically substituted alkoxides capable of forming chelates with palladium and silver ions. The resulting alcogels were dried under vacuum at 423 K, calcined in air at 673 K, and finally reduced in hydrogen at 623 K. Details of the preparation are given in (11–13). Samples are denoted Pd–Ag (67-33), Pd–Ag (50-50), Pd–Ag (33-67), and Ag (100) (numbers in brackets refer to the overall atomic composition in the sample).

II. Catalyst Characterization

The surface of Pd–Ag bimetallic particles in catalysts Pd–Ag (67-33), Pd–Ag (50-50), and Pd–Ag (33-67) is examined through a combination of various characterization results coming from X-ray diffraction (XRD), transmission electron microscopy (TEM), and carbon monoxide chemisorption. In order to be able to calculate the metal dispersion from CO chemisorption, it is of great importance to precisely know the real metals contents in the catalysts. These contents were determined from inductively coupled plasma atomic emission spectroscopy (ICP-AES).

The XRD patterns were obtained with hand-pressed samples mounted on a Philips PW1050 goniometer. A copper anode X-ray tube (Philips PW1729) was used as the radiation source.

TEM analyses were performed on a Siemens Elmiskop 102 transmission electron microscope. Suitable transmission samples were prepared by means of impregnation of the xerogels with an epoxy resin (eurepox 710) to which an amine was added to serve as a hardener. Hardening went on for 48 h after which a 60-nm slice was cut up with a Reichert Supernova ultramicrotome.

Real palladium and silver contents in the catalysts were measured by ICP-AES on a Spectroflam from Spectro Analytical Instruments. Samples were dissolved in concentrated acids (18 mol liter^{-1} H_2SO_4, 22 mol liter^{-1} HF, 14 mol liter^{-1} HNO_3). Pd and Ag contents were obtained by comparison with standard solutions in the same medium.

A volumetric static method was used for CO chemisorption (14). Measurements were obtained on a Fisons Sorptomatic 1990 equipped with a turbomolecular vacuum pump which allows it to reach a high vacuum of 10^{-6} kPa. A sample was placed in a Pyrex bulb connected to two stopcocks which allows hydrogen to flow through the catalyst bed for pretreatment. During the various pretreatment steps, the sample holder was placed in temperature-programmed ovens. During adsorption measurements, it was plunged in a 303 K thermostatically controlled water bath. For each analysis, the sample holder was loaded with about 0.4 g of nonreduced catalyst. Prior to adsorption measurements, the catalyst was reduced and outgassed *in situ* according to the following procedure: under 0.037 mmol s^{-1} flowing hydrogen, the sample was heated to 623 K at a rate of 300 K h^{-1} and was maintained at this temperature for 3 h, after which it was naturally cooled to ambient temperature. The sample holder filled with hydrogen was then transferred to the outgassing unit, where the catalyst was heated under vacuum at a rate of 300 K h^{-1} up to 613 K, maintained at 613 K and 10^{-6} kPa for 16 h, and naturally cooled to ambient temperature. The sample holder maintained under vacuum was finally transferred to the measurements unit, where it was plunged in a water bath at 303 K. In order to examine the influence of the outgassing temperature on the bimetallic particles' surface composition, a second measurements campaign was conducted with fresh samples pretreated according to a procedure which was similar to the one described above but in which the outgassing temperature was 673 K instead of 613 K. So as to distinguish between the two types of pretreatments, the sample name will be followed by the outgassing temperature in brackets (e.g., Pd–Ag (67-33) (613 K)).

Carbon monoxide adsorption was performed at 303 K. A first CO adsorption isotherm was achieved so as to measure the total amount of adsorbed carbon monoxide (chemisorbed + physisorbed). The catalyst was then outgassed on the measurements unit at 303 K for 2 h in a vacuum of 10^{-6} kPa, and a second CO adsorption isotherm was measured in order to evaluate the amount of physisorbed CO.

RESULTS

I. Palladium and Silver Contents in the Catalysts

The experimental palladium and silver contents in samples Pd–Ag (67-33), Pd–Ag (50-50), Pd–Ag (33-67), and Ag (100) measured by ICP-AES are given in Table 1, where

TABLE 1

Pd and Ag Contents

	Nominal contents			Contents determined by ICP-AES		
Catalyst	Pd (wt%)	Ag (wt%)	Pd/(Pd + Ag) (at.%)	Pd (wt%)	Ag (wt%)	Pd/(Pd + Ag) (at.%)
Pd–Ag (67-33)	1.5	0.75	67	2.2	1.1	67
Pd–Ag (50-50)	1.5	1.5	50	2.3	2.2	51
Pd–Ag (33-67)	1.5	3.0	33	1.9	3.7	34
Ag (100)	0	1.5	100	0	1.7	100

they are compared with nominal values calculated from synthesis parameters which can be found in (11). In all xerogels, real metal contents determined from ICP-AES are higher than nominal values. However, the weight ratio Pd/(Pd + Ag), which is equal to the atomic ratio since Pd and Ag have nearly identical atomic weights, calculated with values given by ICP-AES remains identical to the nominal ratio. It can then be concluded that the real metals contents are higher than the nominal contents because of a loss, during gel drying, of unreacted tetraethoxysilane (TEOS), which is the precursor of the silica support.

II. Carbon Monoxide Chemisorption on Bimetallic Catalysts

Around room temperature, CO adsorption on supported metal catalysts leads generally to both chemisorption and physisorption (14, 15). Chemisorption results from a strong interaction which leads to the formation of a real chemical bond between the catalyst and CO molecules, and physisorption results from a weak van der Waals interaction (16). In contrast with chemisorption, which generally occurs on specific metallic sites, physisorption occurs on both metal and support. In order to study the metal particles surface of Pd–Ag/SiO_2 catalysts from CO adsorption data, it is essential to measure the amount of CO chemisorbed on metallic sites. In other words, one must be able to separate chemisorption and physisorption effects.

The method used in the present study to obtain this amount of chemisorbed CO is illustrated in Fig. 1. This method, frequently encountered in the literature, was initially developed by Emmett and Brunauer in their work relative to CO chemisorption on iron catalysts for ammonia synthesis (15, 17–21). The first isotherm, measured immediately after the pretreatment (reduction + outgassing), gives the total amount of adsorbed carbon monoxide: chemisorbed CO + physisorbed CO. To evaluate the amount of physisorbed CO, a second isotherm is measured after a 2-h outgassing at the measurement temperature. Since the interaction between the catalyst and physisorbed molecules is much weaker than the interaction between the catalyst and chemisorbed molecules, the aim of the 2-h outgassing at 303 K is to eliminate as quantitatively as possible physisorbed CO while maintaining chemisorbed CO at the surface of metallic sites. The choice of the outgassing time before the measurement of the second isotherm results from a compromise. Various outgassing times between first and second isotherms can be found in the literature. For example, in their study relative to dispersion of supported palladium catalysts measured by CO adsorption at 293 K, Scholten and van Montfoort (15) measure the CO physisorption isotherm after a 0.5-h outgassing at 293 K. With the Pd–Ag/SiO_2 catalysts examined here, preliminary measurements of the second isotherm after outgassing times of 0.5, 1, 2, and 20 h showed that the same result is obtained, to within experimental error, in the three first cases. On the other hand, after the 20-h outgassing, chemisorbed as well as physisorbed CO are eliminated since the second isotherm is nearly identical to the first one. Consequently, it can be reasonably assumed that with the three first outgassing times, weakly adsorbed CO, that is, physisorbed CO, is quantitatively eliminated, whereas strongly adsorbed CO, that is, chemisorbed CO, remains adsorbed on the metal surface and that the second isotherm corresponds to physisorption only. The outgassing time of 2 h chosen in this study seems then to be appropriate to measure physisorption isotherms, and the reproducibility of those isotherms was checked by performing successive outgassing–adsorption cycles.

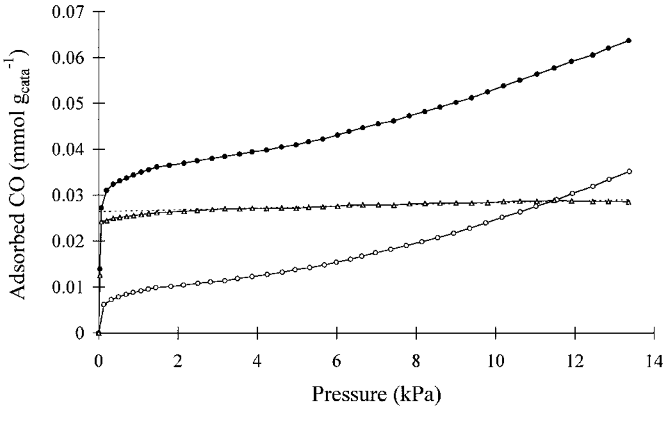

FIG. 1. CO adsorption isotherms at 303 K on catalyst Pd–Ag (67-33) (673 K): (●) first isotherm, chemisorption + physisorption; (○) second isotherm after outgassing at 303 K for 2 h, physisorption; (△) first isotherm–second isotherm, chemisorption; (- - -) regression on the linear part of the chemisorption isotherm.

The chemisorption isotherm is obtained by subtracting the second isotherm from the first one. In theory, when pressure increases, chemisorption isotherms exhibit a linear horizontal region which is pressure independent. This region corresponds to the covering of metallic sites exhibiting a strong interaction with CO (strong sites) by a monolayer, that is, to the saturation of those specific metallic sites with carbon monoxide. However, it is common to obtain experimental chemisorption isotherms in which the saturation linear region is not perfectly horizontal but exhibits a slight slope (14). In that case, a common practice to obtain an estimate of the monolayer uptake is to back-extrapolate the linear region to evaluate the intercept on the uptake axis (14, 17, 21, 22). This back-extrapolation corresponds to the regression dotted line in Fig. 1. The intercept on the uptake axis gives a good estimation of the amount of CO adsorbed in the form of a monolayer on strong sites. In the case of sample Pd–Ag (67-33) (673 K) in Fig. 1, the slope of the linear region of the chemisorption isotherm is practically

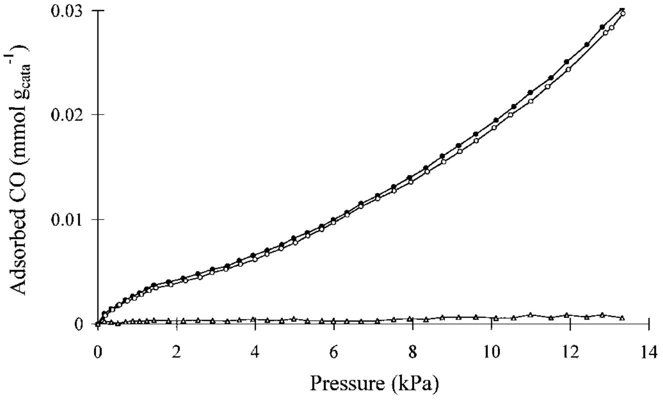

FIG. 2. CO adsorption isotherms at 303 K on catalyst Ag (100) (613 K): (●) first isotherm; (○) second isotherm after outgassing at 303 K for 2 h; (△) first isotherm–second isotherm.

equal to zero. With the other samples, this slope is, in some cases, more pronounced (see Fig. 3).

To study the surface of Pd–Ag bimetallic particles in catalysts Pd–Ag (67-33), Pd–Ag (50-50), and Pd–Ag (33-67) by means of carbon monoxide chemisorption, it is essential to know if CO is chemisorbed on both palladium and silver or only selectively on one of these two metals. CO chemisorption on monometallic palladium catalysts is a well-known phenomenon widely used to measure the Pd dispersion (2, 4, 15–17, 20, 23–26). On the other hand, according to the literature, pure silver does not chemisorb CO (2, 4, 16, 22, 23). This absence of strong interaction between carbon monoxide and Ag has been checked experimentally through the measurement of CO adsorption isotherms on monometallic silver catalyst Ag (100) according to the above-described method. These isotherms are given in Fig. 2. One notices that the second isotherm, which is measured after the outgassing of 2 h at 303 K and which corresponds to physisorption, is nearly equal to the first isotherm. Chemisorption, which is the difference between the two isotherms, is then nonexistent on catalyst Ag (100), which is in agreement with the literature. This result shows also that there is no strong interaction between the silica xerogel support and carbon monoxide, which confirms the generally accepted view according to which chemisorption does not occur on the support.

Since, in monometallic catalysts Pd/SiO_2 and Ag/SiO_2, CO chemisorption occurs on palladium but not on silver, it will be assumed that on the surface of alloy particles in Pd–Ag/SiO_2 bimetallic catalysts, CO chemisorption occurs on palladium atoms only (5). This hypothesis is supported by the work of Soma-Noto and Sachtler (4), who examined the chemisorption of CO on Pd/SiO_2, Ag/SiO_2, and Pd–Ag/SiO_2 catalysts by means of infrared spectroscopy. No IR absorption band which would correspond to a possible bond between carbon monoxide and silver is detected, neither on pure Ag nor on Pd–Ag alloys. In contrast, absorption bands corresponding to bonds between CO and Pd are found with Pd–Ag alloys.

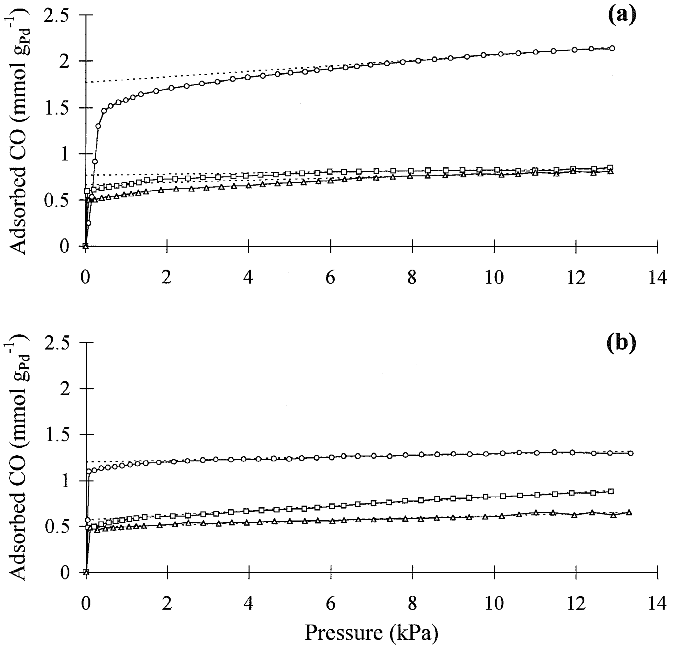

FIG. 3. CO chemisorption isotherms at 303 K on bimetallic Pd–Ag/SiO_2 catalysts: (a) catalysts outgassed at 613 K; (b) catalysts outgassed at 673 K; (○) catalyst Pd–Ag (67-33); (□) catalyst Pd–Ag (50-50); (△) catalyst Pd–Ag (33-67); (---) regression on the linear part of the isotherm.

Chemisorption isotherms of carbon monoxide at 303 K obtained by the subtraction method illustrated in Fig. 1 were determined on bimetallic samples Pd–Ag (67-33), Pd–Ag (50-50), and Pd–Ag (33-67) which were pretreated under vacuum at 613 K, on the one hand, and at 673 K, on the other hand (see Experimental). Those isotherms are presented in Fig. 3. Since chemisorption occurs on palladium only and Pd contents given by ICP-AES differ from one bimetallic catalyst to another (Table 1), the amounts of chemisorbed CO are from now on given in mmol g_{Pd}^{-1} in order to make the comparison between samples easier. The monolayer uptakes, $n_{s,m}$, given by back-extrapolation are listed in Table 2. One observes that the amount of chemisorbed CO related to the weight of Pd, $n_{s,m}$, decreases from sample Pd–Ag (67-33) to sample Pd–Ag (33-67). For

TABLE 2

CO Chemisorption at 303 K on Bimetallic Pd–Ag/SiO_2 Catalysts

Catalyst	Chemisorbed amount $n_{s,m}$ (mmol g_{Pd}^{-1}) Outgassing at 613 K	Chemisorbed amount $n_{s,m}$ (mmol g_{Pd}^{-1}) Outgassing at 673 K
Pd–Ag (67-33)	1.77	1.20
Pd–Ag (50-50)	0.77	0.57
Pd–Ag (33-67)	0.66	0.49

each catalyst, this amount is lower when the pretreatment under vacuum occurs at 673 K instead of 613 K.

III. Calculation of the Pd–Ag Alloy Particles' Surface Composition

Let us immediately specify that we consider here only palladium and silver atoms which are present in alloy particles in catalysts Pd–Ag (67-33), Pd–Ag (50-50), and Pd–Ag (33-67). Silver atoms present in pure Ag particles (11) are not taken into account in the developments below. Moreover, in agreement with results presented in (11), it is assumed that palladium is present only in the form of a Pd–Ag alloy.

One tries to find the fraction $x_{\mathrm{Pd_s}}$ of palladium atoms present at the surface of Pd–Ag alloy particles,

$$x_{\mathrm{Pd_s}} = \frac{n_{\mathrm{Pd_s}}}{n_{\mathrm{Pd_s}} + n_{\mathrm{Ag_s}}}, \qquad [1]$$

where $n_{\mathrm{Pd_s}}$ is the number of Pd atoms at the surface of Pd–Ag alloy particles and $n_{\mathrm{Ag_s}}$ is the number of Ag atoms at the surface of Pd–Ag alloy particles.

The fraction of palladium atoms at the surface, $x_{\mathrm{Pd_s}}$, can be deduced, for catalysts Pd–Ag (67-33), Pd–Ag (50-50), and Pd–Ag (33-67), from a combination of CO chemisorption results given in Table 2 with results coming from X-ray diffraction (XRD) and transmission electron microscopy (TEM). Indeed, expression [1] of $x_{\mathrm{Pd_s}}$ can be developed as

$$x_{\mathrm{Pd_s}} = \frac{n_{\mathrm{Pd_s}}}{n_{\mathrm{Pd}}} \frac{n_{\mathrm{Pd}}}{n_{\mathrm{Pd}} + n_{\mathrm{Ag}}} \frac{n_{\mathrm{Pd}} + n_{\mathrm{Ag}}}{n_{\mathrm{Pd_s}} + n_{\mathrm{Ag_s}}} = D_{\mathrm{Pd}} x_{\mathrm{Pd}} \frac{1}{D_{\mathrm{Pd-Ag}}}, \qquad [2]$$

where n_{Pd} is the total number of Pd atoms in Pd–Ag alloy particles and n_{Ag} is the total number of Ag atoms in Pd–Ag alloy particles.

The first factor in expression [2], $D_{\mathrm{Pd}} = (n_{\mathrm{Pd_s}}/n_{\mathrm{Pd}})$, is the palladium dispersion, that is, the ratio between the number of surface Pd atoms ($\mathrm{Pd_s}$) and the total number of Pd atoms in the catalyst. The second factor, $x_{\mathrm{Pd}} = n_{\mathrm{Pd}}/(n_{\mathrm{Pd}} + n_{\mathrm{Ag}})$, is the fraction of Pd atoms in the Pd–Ag alloy particles. This fraction corresponds to the bulk composition of alloy particles. The third factor, $(1/D_{\mathrm{Pd-Ag}}) = (n_{\mathrm{Pd}} + n_{\mathrm{Ag}})/(n_{\mathrm{Pd_s}} + n_{\mathrm{Ag_s}})$, is the inverse of the overall dispersion of the alloy particles with no distinction between the two metals, that is, the ratio between the total number of metal atoms in Pd–Ag alloy particles and the number of metal atoms at the surface of those particles. The D_{Pd}, x_{Pd}, and $D_{\mathrm{Pd-Ag}}$ are estimated below by CO chemisorption, XRD, and TEM, respectively.

Calculation of the palladium dispersion D_{Pd} from CO chemisorption. Results in Table 2 allow us to calculate the palladium dispersion D_{Pd} thanks to Eq. [3]: (17),

$$D_{\mathrm{Pd}} = n_{\mathrm{s,m}} M_{\mathrm{Pd}} X_{\mathrm{Pd-CO}} \times 10^{-3}. \qquad [3]$$

Here, $n_{\mathrm{s,m}}$ is the amount of CO needed to form a chemisorbed monolayer on palladium sites (mmol $\mathrm{g_{Pd}^{-1}}$); M_{Pd} is the atomic weight of palladium, 106.42 g $\mathrm{mol^{-1}}$; and $X_{\mathrm{Pd\text{–}CO}}$ is the chemisorption mean stoichiometry, that is, the mean number of Pd atoms on which one CO molecule is adsorbed.

To be able to use relation [3], the chemisorption mean stoichiometry $X_{\mathrm{Pd\text{–}CO}}$ must then be determined for catalysts Pd–Ag (67-33), Pd–Ag (50-50), and Pd–Ag (33-67). Carbon monoxide can adsorb on palladium in various configurations. One CO molecule can be bound to either only one surface atom $\mathrm{Pd_s}$ (linear CO) or several (two, three, or four) atoms $\mathrm{Pd_s}$ (multicenter CO) (2, 5, 15, 25). Studies on monometallic catalysts Pd/$\mathrm{SiO_2}$ showed that the ratio between linear CO and multicenter CO increases with Pd dispersion (27, 28). This leads to a decrease of the chemisorption mean stoichiometry $X_{\mathrm{Pd\text{–}CO}}$ when dispersion increases (29). Soma-Noto and Sachtler (4) studied infrared spectra of carbon monoxide chemisorbed on Pd–Ag alloy particles supported on silica. According to these authors, CO chemisorption occurs on palladium atoms only, which is in agreement with CO adsorption measurements on bimetallic catalysts Pd–Ag (67-33), Pd–Ag (50-50), and Pd–Ag (33-67) and monometallic silver catalyst Ag (100). IR spectra of CO adsorbed on Pd–Ag alloy particles of various bulk compositions (calculated from XRD) obtained by Soma-Noto and Sachtler allow us to examine the relative abundance of linear and multicenter CO chemisorbed on Pd. Three CO absorption bands are observed on palladium and on Pd–Ag alloys at around 2060, 1960, and 1920 $\mathrm{cm^{-1}}$. Frequencies of these absorption bands remain almost unchanged from pure Pd to Pd–Ag alloys with increasing Ag contents. In contrast, the relative intensities of these bands change radically. The band at 2060 $\mathrm{cm^{-1}}$, which corresponds to linear CO (25) and the intensity of which is weak with pure palladium, becomes the most intense with Pd–Ag alloys. On the other hand, bands at 1960 and 1920 $\mathrm{cm^{-1}}$, corresponding to multicenter CO (25) and which are dominant with pure Pd, disappear almost completely beyond 25 at.% of silver in the bulk of the alloy.

In conclusion, the introduction of silver in palladium reduces strongly the presence of multicenter CO in relation to linear CO, which becomes almost the only species beyond 25 at.% of silver in the bulk of the alloy. In bimetallic catalysts Pd–Ag (67-33), Pd–Ag (50-50), and Pd–Ag (33-67), the silver contents in alloy particles are higher than 30 at.% (XRD results given in (11) and in Table 3). It can then be admitted that CO is chemisorbed on palladium in the linear form only. As a consequence, a stoichiometry $X_{\mathrm{Pd\text{–}CO}} = 1$ will be used for the calculation of the palladium dispersion, D_{Pd}. Values obtained for D_{Pd}, applying relation [3], are given in Table 3. As for the amounts of chemisorbed CO, $n_{\mathrm{s,m}}$, in Table 2, to which values of D_{Pd} are proportional (relation [3]), it is observed that D_{Pd} decreases from Pd–Ag (67-33) to Pd–Ag (33-67). For one catalyst, D_{Pd} is

TABLE 3

Calculation of the Surface Composition of Pd–Ag Alloy Particles

	XRD		TEM			Outgassing at 613 K		Outgassing at 673 K	
Catalyst	x_{Pd} (at.%)	d_{XRD} (nm)	d_S (nm)	D_{Pd-Ag} (%)	d_V (nm)	D_{Pd} (%)	x_{Pd_s} (at.%)	D_{Pd} (%)	x_{Pd_s} (at.%)
Pd–Ag (67-33)	69	1.9	2.8	41	2.9	19	31.6	13	21.4
Pd–Ag (50-50)	57	2.1	3.3	35	3.4	8	13.3	6	9.8
Pd–Ag (33-67)	54	2.0	3.8	30	4.0	7	12.6	5	9.2

Note. Here x_{Pd}, is the fraction of Pd atoms in the bulk of Pd–Ag alloy particles estimated from XRD; d_{XRD} is the mean size of Pd–Ag particles estimated from X-ray line broadening; d_S is the mean surface diameter of Pd–Ag alloy particles, $\sum n_i d_i^3 / \sum n_i d_i^2$, estimated from TEM; D_{Pd-Ag} is the overall dispersion of Pd–Ag alloy particles estimated from TEM; d_V is the mean volume diameter of Pd–Ag alloy particles, $\sum n_i d_i^4 / \sum n_i d_i^3$, estimated from TEM; D_{Pd} is the Pd dispersion estimated from CO chemisorption; x_{Pd_s} is the fraction of Pd atoms present at the surface of Pd–Ag alloy particles estimated from the combination of CO chemisorption, XRD, and TEM results.

lower when the vacuum pretreatment is performed at 673 K instead of 613 K.

Calculation of the Pd atoms fraction x_{Pd} in the bulk of alloy particles from XRD. XRD results obtained with samples Pd–Ag (67-33), Pd–Ag (50-50), and Pd–Ag (33-67) are presented and discussed in detail in the first paper of this series (11). Some of these results are reviewed here. Figure 4 shows the diffractograms obtained for the three bimetallic samples. Between the (111) Bragg lines of pure Pd and Ag, these xerogels exhibit a broad peak which indicates the presence of a solid solution (SS) in the form of small Pd–Ag alloy particles. After spectra deconvolution, as shown in Fig. 5 for the case of sample Pd–Ag (50-50), the (200) broad peak appears. The presence of unalloyed silver is clearly evident in sample Pd–Ag (33-67), two peaks being characteristic of this metal (Fig. 4). In xerogels Pd–Ag (67-33) and Pd–Ag (50-50), the presence of pure silver is also demonstrated by the shoulder at the left of the (111) SS peak and the small (200) Ag peak (Figs. 4 and 5). The composition of the solid solution was calculated from the unit cell parameter corresponding to the SS peak (30). This composition is given in Table 3 in the form of the fraction x_{Pd} of Pd atoms in the bulk of bimetallic particles. The very wide SS peaks are due to the small size of the particles and/or to a distribution of composition (31). Assuming that all the bimetallic particles have the same Pd–Ag composition, their size can be calculated from the peak broadening and Scherrer's formula (17, 30). Bimetallic particles in xerogels Pd–Ag (67-33), Pd–Ag (50-50), and Pd–Ag (33-67) are found to be finely dispersed: their size d_{XRD} is about 2 nm (Table 3). As shown in (11), according to XRD

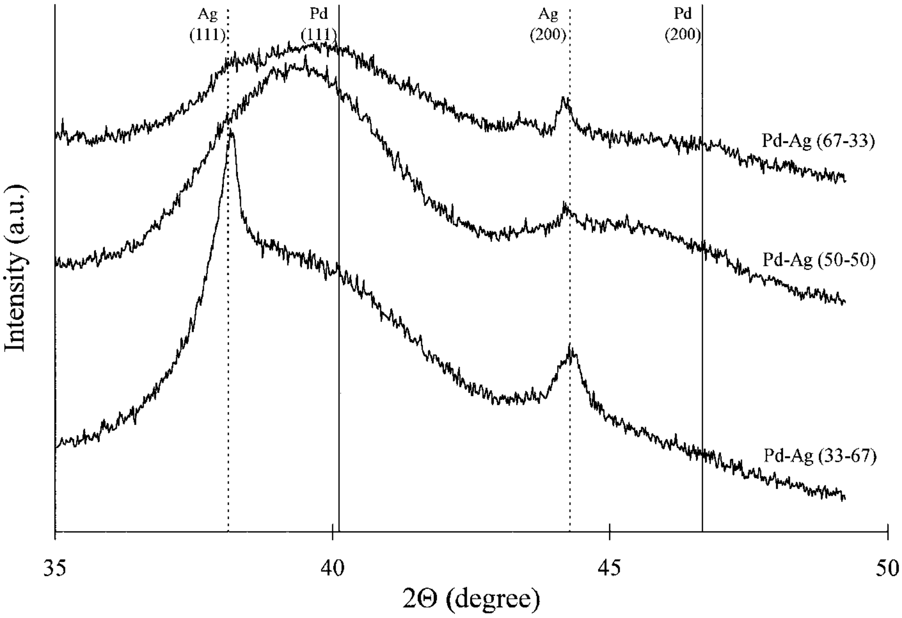

FIG. 4. X-ray diffraction patterns of Pd–Ag/SiO$_2$ catalysts.

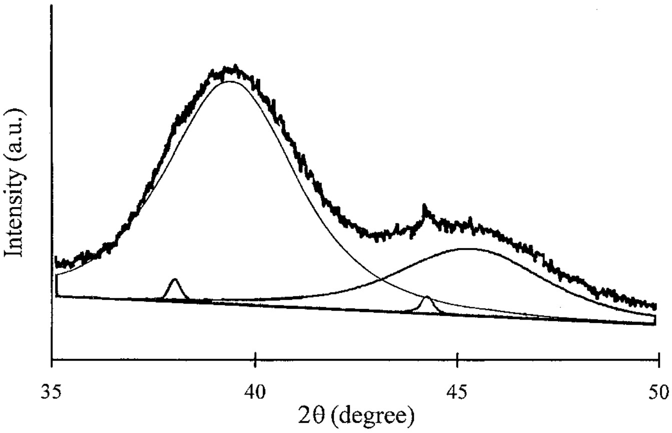

FIG. 5. Deconvolution into four peaks of the XRD pattern of sample Pd–Ag (50-50).

results, pure silver particles in these samples exceed 10 nm and are then much larger.

Calculation of the overall dispersion $D_{\mathrm{Pd\text{-}Ag}}$ of alloy particles from TEM. The overall dispersion $D_{\mathrm{Pd\text{-}Ag}}$, that is, the ratio between the number of metal atoms at the surface of the Pd–Ag alloy particles and the total number of metal atoms in those particles, is given by (17)

$$D_{\mathrm{Pd\text{-}Ag}} = \frac{6(v_{\mathrm{m}}/a_{\mathrm{m}})}{d_{\mathrm{S}}} \quad \text{with } d_{\mathrm{S}} = \frac{\sum n_i d_i^3}{\sum n_i d_i^2}, \qquad [4]$$

where v_{m} is the mean volume occupied by a metal atom in the bulk of the alloy (nm^3), a_{m} is the mean surface area occupied by a surface metal atom (nm^2), d_{S} is the mean surface diameter of Pd–Ag alloy particles (nm), n_i is the number of alloy particles of a given diameter d_i, d_i is the alloy particles diameter (nm).

For palladium and silver, the values of v_{m} are 0.01470 and 0.01706 nm^3, respectively, and the values of a_{m} are 0.0793 and 0.0875 nm^2, respectively (17). Note that the values of a_{m} were obtained assuming equal proportions of crystallographic planes (100), (110), and (111) at the surface of metal particles.

For each catalyst, the mean surface diameter d_{S} is calculated from the diameters d_i of 30 particles. These diameters are measured manually on TEM micrographs, an example of which is given in Fig. 6 with catalyst Pd–Ag (33-67). The large metal particles in the range 7 to 10 nm observed on those micrographs are not taken into account since, according to results published in (11), they correspond to pure silver particles and not to Pd–Ag alloy particles. Values of d_{S} obtained with catalysts Pd–Ag (67-33), Pd–Ag (50-50), and Pd–Ag (33-67) are given in Table 3. From these values, the overall dispersion $D_{\mathrm{Pd\text{-}Ag}}$ of the alloy particles is calculated by means of relation [4]. The values taken for v_{m} and a_{m} are arithmetic means of values given above for Pd and Ag, that is, $v_{\mathrm{m}} = 0.01588$ nm^3 and $a_{\mathrm{m}} = 0.0834$ nm^2. The values of $D_{\mathrm{Pd\text{-}Ag}}$ are given in Table 3.

Let us make here a brief comment about the particle sizes given by XRD and TEM. According to (17), since XRD is sensitive to the volume of particles, the mean crystallite size d_{XRD} estimated from X-ray line broadening and Scherrer's formula corresponds to a volume weighted average diameter $\sum n_i d_i^4 / \sum n_i d_i^3$. In order to compare d_{XRD} with TEM results, a mean volume diameter $d_{\mathrm{V}} = \sum n_i d_i^4 / \sum n_i d_i^3$ must then be calculated from TEM micrographs. For each catalyst, d_{V} has been calculated from the diameters d_i of the same 30 particles used for the calculation of d_{S}. Results are given in Table 3. A comparison between d_{XRD} and d_{V} indicates that the size obtained by diffraction is systematically lower than the one obtained by microscopy. As mentioned in the above section dedicated to the calculation of x_{Pd} from XRD, this might indicate that the broadening of XRD peaks corresponding to the solid solution results not only from the small size of the particles but also from a distribution of composition (31). As a consequence, the sizes calculated from XRD would be underestimated.

It is useful to remark that it could be tempting to assimilate d_{XRD} to d_{S} in relation [4] and calculate $D_{\mathrm{Pd\text{-}Ag}}$ from XRD instead of TEM. Indeed, d_{XRD} should theoretically correspond to d_{V}, and values of d_{V} are close to values of d_{S} (Table 3), which indicates that the particle size distribution is narrow. However, because of the above-mentioned probable composition distribution, d_{XRD} is a biased estimate of $\sum n_i d_i^4 / \sum n_i d_i^3$ and does not correspond to d_{V}. As a consequence, d_{XRD} is not suitable for the calculation of $D_{\mathrm{Pd\text{-}Ag}}$.

One has now the values of palladium dispersion, D_{Pd}, palladium atomic fraction in the bulk of Pd–Ag alloy particles, x_{Pd}, and overall dispersion of alloy particles, $D_{\mathrm{Pd\text{-}Ag}}$. It is then possible to calculate the surface composition $x_{\mathrm{Pd_s}}$, that is, the fraction of palladium atoms at the surface of the Pd–Ag alloy particles, via relation [2]. An implicit assumption, which is necessary for the calculation of $x_{\mathrm{Pd_s}}$, must be specified, however. Values of x_{Pd} and $D_{\mathrm{Pd\text{-}Ag}}$ were obtained by XRD and TEM with samples of catalysts Pd–Ag (67-33), Pd–Ag (50-50), and Pd–Ag (33-67) immediately after calcination at 673 K and reduction at 623 K (11). On the other hand, values of D_{Pd} were obtained with samples calcined and reduced under the same conditions, but these samples were moreover outgassed for 16 h at either 613 K or 673 K (see Experimental), due to reasons characteristic of CO chemisorption. In the method for determining the surface composition presented in this paper, it is assumed that the outgassing modifies neither the bulk composition of the alloy particles, x_{Pd}, nor their size, nor hence their overall dispersion $D_{\mathrm{Pd\text{-}Ag}}$. Values obtained for the surface composition $x_{\mathrm{Pd_s}}$ are given in Table 3. A very marked impoverishment in palladium and hence a very marked enrichment in silver of the Pd–Ag alloy

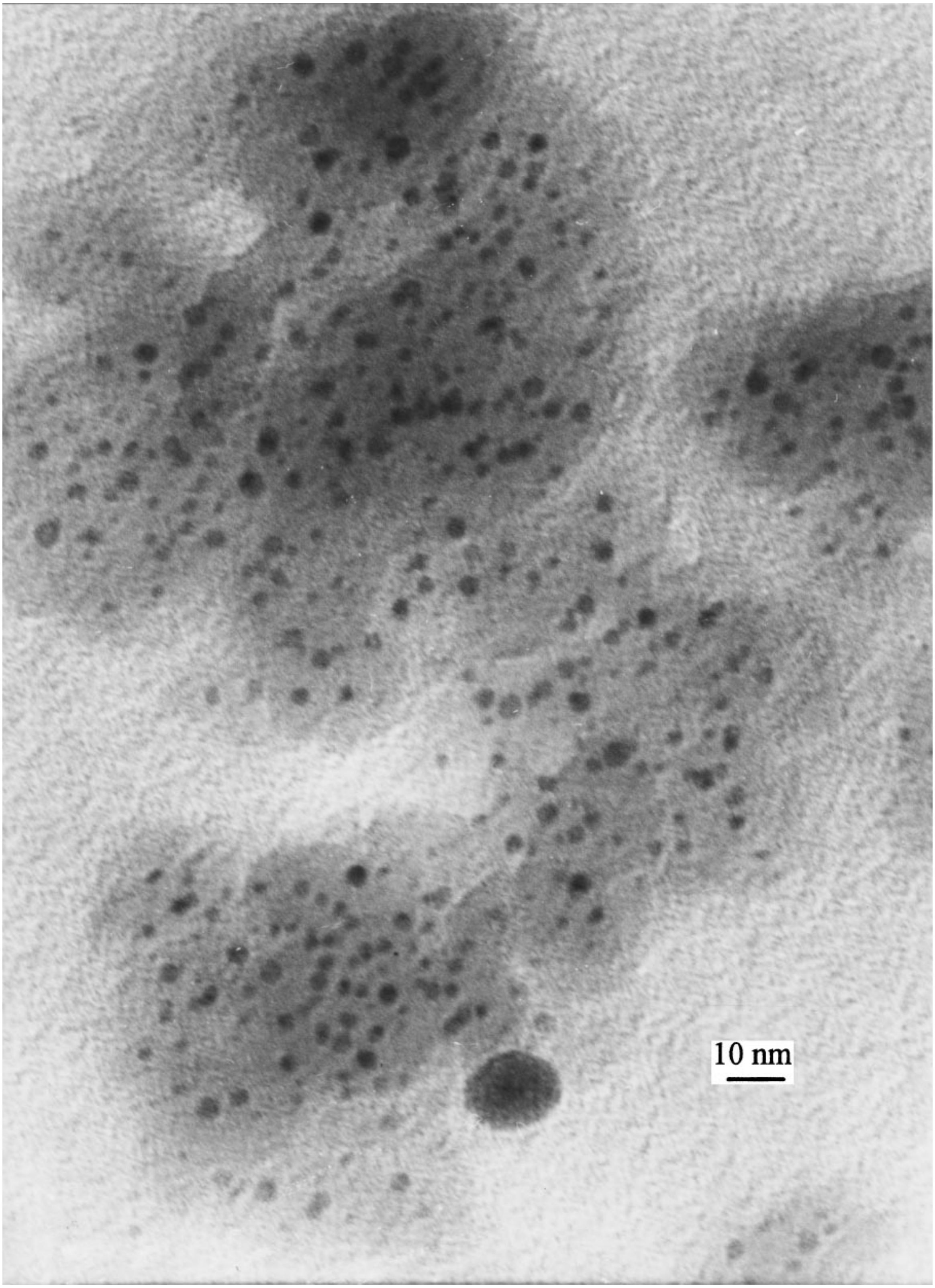

FIG. 6. TEM micrograph of sample Pd–Ag (33-67) (1000000×).

particles surface in relation to their bulk is observed. This composition gap between the surface and the bulk is slightly higher for samples outgassed at 673 K instead of 613 K.

DISCUSSION

Kuijers and Ponec (3) determined the surface composition x_{Pd_s} of bulky Pd–Ag alloys in the form of powder by Auger electron spectroscopy. These authors also calculated x_{Pd_s} from IR spectra of carbon monoxide chemisorbed on Pd–Ag/SiO_2 catalysts obtained by Soma-Noto and Sachtler (4) and by Sachtler (5). Their results, as well as results obtained in the present study, are presented in Fig. 7. In every case, the bulk composition x_{Pd} was estimated by XRD. The dotted lines in Fig. 7 correspond to Auger spectroscopy with bulky alloys. Curve (a) was obtained with Pd–Ag alloys equilibrated under vacuum at 673 K for 16 h. Curve (d) was obtained with the same alloys treated at 670 K for 16 h under 0.013 kPa of CO, and then outgassed at ambient temperature (3). The continuous lines correspond to IR spectroscopy experimental data of CO chemisorbed on Pd–Ag/SiO_2 catalysts (4) interpreted by a theoretical model developed by Sachtler (5). The two curves (b) and (c) correspond to two reasonable extreme values of one parameter λ in this model, which cannot be determined experimentally (3, 5) (see below).

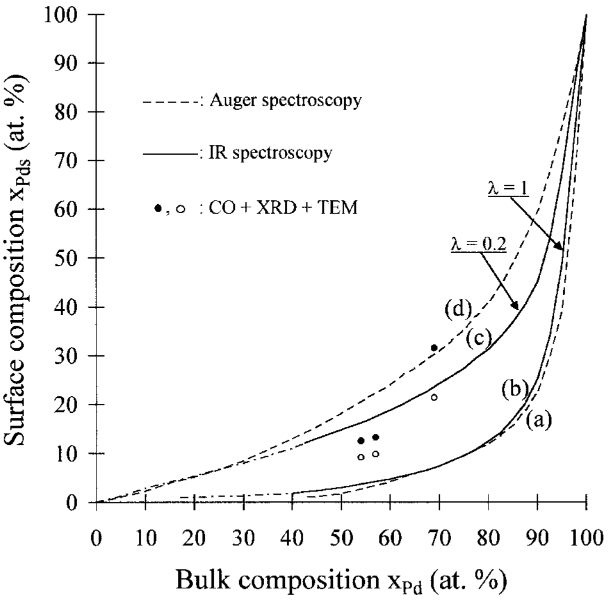

FIG. 7. Comparison of surface compositions of Pd–Ag alloys: (- - -) surface composition determined by Auger spectroscopy with alloys sintered *in vacuo* (a) and after interaction with CO (d); (—) surface composition determined thanks to IR data of adsorbed CO (b and c) (according to Kuijers and Ponec (3)); (circles) surface composition obtained in this study with catalysts Pd–Ag (67-33), Pd–Ag (50-50), and Pd–Ag (33-67) outgassed at 613 K (●) and at 673 K (○). See text for details.

Concerning Auger electron spectroscopy, it is important to point out that the major part of the Auger signal (about 80%) comes from the bulk of the alloy and not from the surface (2, 3). It is, however, only the first atomic layer at the surface of the Pd–Ag alloy whose composition has to be determined. To obtain the surface composition from Auger spectroscopy, it is then crucial to be able to separate the contribution of the external atomic layer from the contributions of internal layers. By evaluating the contribution of the first layer, Kuijers and Ponec (3) obtained surface composition curves (a) and (d), which show a very pronounced enrichment in silver. Their results are in agreement with Auger spectroscopy data obtained by Wood and Wise in an earlier study (6) provided that the same separation between contributions of the external layer and internal layers is performed. However, Kuijers and Ponec (3) point out that, for an unknown reason, their results differ from those obtained by Christmann and Ertl (32), who conclude from Auger spectroscopy results that the surface composition of Pd–Ag alloys is equal to that of the bulk.

Curve (a) relates to Pd–Ag alloys treated under vacuum at 673 K for 16 h. This length of time allows the alloys to reach their equilibrium composition. In other words, with lengths of time for treatment under vacuum at 673 K longer than 16 h, no evolution of the Auger signal is observed. The strong surface enrichment with silver is in agreement with the theoretical prediction according to which, at thermodynamic equilibrium, alloys forming a solid solution (completely miscible metals) exhibit, when under vacuum, a surface enriched with the metal having the lowest surface energy (2, 7). In the case of the Pd–Ag alloy, a surface enrichment with silver whose surface energy is lower than the one of palladium is then to be expected (3, 7, 9). When the alloy is contacted with an adsorbing gas, the thermodynamic equilibrium evolves toward an alloy surface enrichment with the metal having the strongest interaction with the adsorbate (2, 7). This equilibrium shift is illustrated by curve (d), which relates to the surface composition of Pd–Ag alloys treated at 670 K for 16 h with 0.013 kPa of carbon monoxide and subsequently outgassed at ambient temperature. CO interacts strongly with palladium but not with silver (see above), which leads to a surface enrichment with silver which is less marked than the one observed with alloy treated under vacuum.

Figure 7 also shows two curves ((b) and (c)) of surface composition x_{Pd_s} calculated by Kuijers and Ponec (3) from IR band intensities of CO chemisorbed on Pd–Ag/SiO_2 catalysts obtained by Soma-Noto and Sachtler (4) and a theoretical model developed by Sachtler (5). This model links the surface composition x_{Pd_s} to the ratio $q = I_l/(I_l + I_m)$ where I_l and I_m are IR band intensities of linear and multicenter CO, respectively. To obtain curves (b) and (c), Kuijers and Ponec (3) used experimental values of q as a function of the bulk composition x_{Pd} of Pd–Ag alloy particles measured by Soma-Noto and Sachtler (4). They calculated the surface compositions $x_{\mathrm{Pd_s}}$ corresponding to these experimental values of q using Sachtler's model. In this manner, they obtained the relation $x_{\mathrm{Pd_s}} = f(x_{\mathrm{Pd}})$ between the surface compositions $x_{\mathrm{Pd_s}}$ and the bulk composition x_{Pd}. The formula derived by Sachtler (5) comprises one parameter λ which cannot be determined experimentally: $\lambda = \varepsilon_{\mathrm{m}}\theta_{\mathrm{m}}/\varepsilon_{\mathrm{l}}\theta_{\mathrm{l}}$, where ε stands for IR specific absorbance and θ stands for coverage of palladium sites (at given pressure) for the linear (l) and multiple (m) coordinated species (3). According to Sachtler (5), the coverage of Pd sites for the multiple coordinated species, θ_{m}, that is, the number of CO molecules adsorbed in the multicenter form divided by the number of surface palladium atoms involved in such complexes, may be smaller than θ_{l}. Moreover, the specific absorbance of the linear complex ε_{l} exceeds the specific absorbance ε_{m} of the multisite complex by a factor 2 or 3, in accordance with the literature data on mono- and binuclear metal carbonyls (5, 33, 34). The quotient $\lambda = \varepsilon_{\mathrm{m}}\theta_{\mathrm{m}}/\varepsilon_{\mathrm{l}}\theta_{\mathrm{l}}$ may therefore be considerably smaller than unity. According to Kuijers and Ponec (3), it is reasonable to estimate λ as being between, say 0.2 and 1. Curves (b) and (c) correspond to these two extreme values. It is interesting to note that these two curves are situated between curves (a) and (d), obtained by Auger spectroscopy and which correspond to extreme cases. Curve (a) corresponds indeed to alloy powders equilibrated under vacuum at 673 K for 16 h, whereas curve (d) corresponds to alloy powders treated with CO at 670 K for 16 h. Curves (b) and (c) correspond to supported Pd–Ag alloys immersed in a CO atmosphere at ambient temperature during IR spectrum recording. According to Bouwman *et al.* (7), the shift of thermodynamic equilibrium in favor of an alloy surface enrichment with palladium, resulting from the affinity between Pd and CO and requiring Pd atom diffusion toward the surface, occurs from ambient temperature. In consequence, curves (b) and (c) reflect probably a partial enrichment of the surface with palladium, which would explain their intermediate situation in relation to curves (a) and (d) (2).

Values of the surface composition obtained by the alternative method proposed in the present study ((●) and (○) in Fig. 7), which combines results from CO chemisorption, XRD, and TEM, are in complete agreement with curves (a), (b), (c), and (d) calculated from Auger and IR spectroscopies. It is observed that, as for curves (b) and (c), the values obtained here are situated between curve (a), calculated from Auger spectroscopy with alloys equilibrated under vacuum at 673 K for 16 h, and curve (d), calculated from Auger spectroscopy with alloys treated under CO at 670 K for 16 h. This can be explained, as for curves (b) and (c), by a partial enrichment of the surface of Pd–Ag particles with palladium during CO chemisorption isotherm measurements at 303 K due to the affinity between Pd and CO.

The palladium fraction at the surface of alloy particles seems to be slightly lower in samples outgassed at 673 K than in samples outgassed at 613 K. A possible reason for this is that, at the end of the 673-K outgassing, alloy particles are closer to thermodynamic equilibrium, which predicts a surface enrichment with silver, since the diffusion of metal atoms inside the alloy, which is necessary to reach equilibrium, is favored when temperature increases.

The experimental method presented in this study allows us to evaluate the surface compositions of alloy particles in catalysts Pd–Ag (67-33), Pd–Ag (50-50), and Pd–Ag (33-67). However, it does not provide any information about the distributions of Pd and Ag atoms on these surfaces enriched with silver. Kok *et al.* (35) applied the Monte Carlo method (2) to simulate the distribution of atoms on a Pd–Ag (111) surface containing 10% of palladium atoms, namely, a surface composition very close to the one observed with samples Pd–Ag (50-50) and Pd–Ag (33-67) (Table 3). The results of this simulation suggest a surface where palladium atoms are isolated by surrounding silver atoms. It can then be assumed that, under the measuring conditions applied in this study, the surface of Pd–Ag alloy particles in catalysts Pd–Ag (50-50) and Pd–Ag (33-67) exhibit a majority of palladium atoms which are individually isolated in the silver matrix.

CONCLUSIONS

When a palladium–silver alloy is contacted with carbon monoxide, CO molecules form chemical bonds with Pd atoms only. Theoretically, CO chemisorption then allows us to selectively titrate palladium on a Pd–Ag surface. However, using this technique only does not allow us to probe the surface composition since it does not provide any information on the silver surface concentration. The combination of results from carbon monoxide chemisorption, X-ray diffraction, and transmission electron microscopy allowed us to calculate the surface composition of the palladium–silver particles in catalysts Pd–Ag (67-33), Pd–Ag (50-50), and Pd–Ag (33-67). Values obtained indicate a very pronounced surface enrichment with silver. This Ag concentration, which is higher at the surface in comparison with the bulk of the alloy, results from a surface energy of silver which is lower than the surface energy of palladium. Surface compositions obtained with this method, which combines three different experimental techniques, have been compared with the literature data obtained, on the one hand, with Pd–Ag alloy powders examined by Auger electron spectroscopy and, on the other hand, with Pd–Ag/SiO_2 catalysts examined by infrared spectroscopy of chemisorbed CO. The results of the three methods show remarkable agreement. They display moreover a Pd surface enrichment induced by carbon monoxide chemisorption which leads to a less marked surface silver enrichment when the alloy is contacted with carbon monoxide. An influence of pretreatment temperature on surface composition is observed. Indeed, the temperature must be sufficiently high and must be maintained for a sufficiently long time to allow the alloys to approach thermodynamic equilibrium through diffusion of Pd and Ag atoms between the bulk and the surface of the crystal. In the case of catalysts Pd–Ag (50-50) and Pd–Ag (33-67), exhibiting the highest silver contents, the majority of the palladium surface atoms are, according to the literature data, individually isolated in a silver matrix.

Forthcoming papers of this series will deal with the diffusion of reactants inside the particular porous texture of cogelled xerogel catalysts and with the kinetics and mechanism of hydrodechlorination of 1,2-dichloroethane over the Pd–Ag (33-67) catalyst.

ACKNOWLEDGMENTS

B. Heinrichs is grateful to the Fonds pour la Formation à la Recherche dans l'Industrie et dans l'Agriculture, F.R.I.A., for a Ph.D. grant. The Ministère de la Région Wallonne—Direction Générale des Technologies et de la Recherche, the Service de la Programmation de la Politique Scientifique, and the Belgian Fonds National de la Recherche Scientifique are also gratefully acknowledged for financial support.

REFERENCES

1. Sachtler, W. M. H., and van Santen, R. A., *Adv. Catal.* **26**, 69 (1977).
2. Ponec, V., and Bond, G. C., "Catalysis by Metals and Alloys." Elsevier, Amsterdam, 1995.
3. Kuijers, F. J., and Ponec, V., *J. Catal.* **60**, 100 (1979).
4. Soma-Noto, Y., and Sachtler, W. M. H., *J. Catal.* **32**, 315 (1974).
5. Sachtler, W. M. H., *Catal. Rev. Sci. Eng.* **14**, 193 (1976).
6. Wood, B. J., and Wise, H., *Surf. Sci.* **52**, 151 (1975).
7. Bouwman, R., Lippits, G. J. M., and Sachtler, W. M. H., *J. Catal.* **25**, 350 (1972).
8. Stephan, J. J., Franke, P. L., and Ponec, V., *J. Catal.* **44**, 359 (1976).
9. Tyson, W. R., and Miller, W. A., *Surf. Sci.* **62**, 267 (1977).
10. Wise, H., *J. Catal.* **43**, 373 (1976).
11. Heinrichs, B., Delhez, P., Schoebrechts, J.-P., and Pirard, J.-P., *J. Catal.* **172**, 322 (1997).
12. Heinrichs, B., "L'hydrodéchloration sélective du 1,2-dichloroéthane en éthylène sur des catalyseurs Pd-Ag/SiO_2." Ph.D. thesis, Université de Liège, Liège, 1999.
13. Delhez, P., Heinrichs, B., Pirard, J.-P., and Schoebrechts, J.-P., Demande de brevet européen, EP 0 745 426 A1 (1996).
14. Anderson, J. R., "Structure of Metallic Catalysts." Academic Press, London, 1975.
15. Scholten, J. J. F., and van Montfoort, A., *J. Catal.* **1**, 85 (1962).
16. Scholten, J. J. F., Communication at the "Workshop Micromeritics, Veldhoven, April 5-6, 1993."
17. Bergeret, G., and Gallezot, P., *in* "Handbook of Heterogeneous Catalysis" (G. Ertl, H. Knözinger, and J. Weitkamp, Eds.), Vol. 2, p. 439. Wiley–VCH, Weinheim, 1997.
18. Emmett, P. H., and Brunauer, S., *J. Am. Chem. Soc.* **59**, 310 (1937).
19. Emmett, P. H., and Brunauer, S., *J. Am. Chem. Soc.* **59**, 1553 (1937).
20. Scholten, J. J. F., Pijpers, A. P., and Hustings, A. M. L., *Catal. Rev. Sci. Eng.* **27**, 151 (1985).
21. Iglesia, E., and Boudart, M., *J. Catal.* **81**, 204 (1983).
22. Cormack, D., Pritchard, J., and Moss, R. L., *J. Catal.* **37**, 548 (1975).
23. Foger, K., *in* "Catalysis: Science and Technology" (J. R. Anderson and M. Boudart, Eds.), Vol. 6, p. 227. Springer-Verlag, Berlin, 1984.
24. Boudart, M., and Djéga-Mariadassou, G., "Cinétique des réactions en catalyse hétérogène." Masson, Paris, 1982.
25. Eischens, R. P., Francis, S. A., and Pliskin, W. A., *J. Phys. Chem.* **60**, 194 (1956).
26. Heinrichs, B., Noville, F., and Pirard, J.-P., *J. Catal.* **170**, 366 (1997).
27. Ichikawa, S., Poppa, H., and Boudart, M., *J. Catal.* **91**, 1 (1985).
28. Rieck, J. S., and Bell, A. T., *J. Catal.* **103**, 46 (1987).
29. Joyal, C. L. M., and Butt, J. B., *J. Chem. Soc. Faraday Trans.* **83**, 2757 (1987).
30. Sinfelt, J. H., "Bimetallic Catalysts—Discoveries, Concepts, and Applications." Wiley, New York, 1983.
31. El Hamdaoui, A., Bergeret, G., Massardier, J., Primet, M., and Renouprez, A., *J. Catal.* **148**, 47 (1994).
32. Christmann, K., and Ertl, G., *Surf. Sci.* **33**, 254 (1972).
33. Soma-Noto, Y., and Sachtler, W. M. H., *J. Appl. Phys. Suppl.* **2**, 241 (1974).
34. Noack, K., *Helv. Chim. Acta* **14**, 1847 (1962).
35. Kok, G. A., Noordermeer, A., and Nieuwenhuys, B. E., *Surf. Sci.* **152/153**, 505 (1985).